BJR

https://doi.org/10.1259/bjr.20190249

Received: 07 March 2019 | Revised: 21 August 2019 | Accepted: 27 August 2019

Cite this article as:
Sala F, Dapoto A, Morzenti C, firetto Mcristina, Valle C, Tomasoni A, et al. Bone islands incidentally detected on computed tomography: frequency of enostosis and differentiation from untreated osteoblastic metastases based on CT attenuation value. *Br J Radiol* 2019; **92**: 20190249.

FULL PAPER

Bone islands incidentally detected on computed tomography: frequency of enostosis and differentiation from untreated osteoblastic metastases based on CT attenuation value

[1]FRANCESCO SALA, [2]ANNARITA DAPOTO, [3]C. MORZENTI, [4]MARIA CRISTINA FIRETTO, MD, [5]CLARISSA VALLE, [6]A. TOMASONI and [7]SANDRO SIRONI

[1]Radiologist, ASST Papa Giovanni XXIII, Bergamo,
[2]Radiologist resident, Milano Bicocca University, ASST Papa Giovanni XXIII, Bergamo,
[3]Radiologist, ASST Papa Giovanni XXIII, Bergamo,
[4]Radiologist, Ca' Granda IRCSS Maggiore Policlinico Hospital Foundation Trust, Milano,
[5]Radiologist resident, Milano Bicocca University, ASST Papa Giovanni XXIII, Bergamo,
[6]Radiologist, ASST Papa Giovanni XXIII, Bergamo,
[7]Professor of Radiology, Milano Bicocca University, ASST Papa Giovanni XXIII, Bergamo,

Address correspondence to: Dr Maria cristina firetto
E-mail: *firettomariacristina@gmail.com*

Objective: The frequency of enostosis incidentally found on CT and CT attenuation value to distinguish them from untreated osteoblastic metastases (UOM).
Methods: Enostosis group: 46 polytrauma patients underwent thoracoabdominal CT. Inclusion criteria: age range 14–35 years. Exclusion criteria: cancer, previous fractures. UOM group: 20 patients with radiological diagnosis of UOM. Analyzed data: number, size, location and density of enostoses and metastases. The density was measured with the broadest possible region of interest at the center of the lesion by two radiologists independently. Receiver operatingcharacteristic analysis to determine the sensitivity and specificity, area under the curve 95% confidence intervals and cutoff values of CT density to differentiate metastases from enostoses.
Results: Patients were 28 ± 7 years old (72% males). 41 (89%) patients had 124 enostoses (2–15 mm) with an average density of 1007 ± 122 Hounsfiled unit (HU, observer1) and 1052 ± 107 (observer2). The most common sites of occurrence were the proximal femur (34%), the pelvis (22%), the acetabulum (20%), the proximal humerus (11%), the vertebrae (11%) and the rib (2%). 13 patients had 1 bone island, 8 patients had 2, 9 cases had 3 and 11 cases had more than 3 enostoses. Overall, 114 UOM were evaluated, their average density was 728 ± 163 HU (observer1) and 712 ± 178 HU (observer2). The area under the curve value of mean density to distinguish enostoses from UOM was 0,982. Using a cut-off of 881 HU for mean density, sensitivity was 98% and specificity 95%.
Conclusion: The frequency of enostosis in this study is 89%. The average density identified can help to distinguish enostoses from UOM.
Advances in knowledge: We report the exact frequency of enostosis.

INTRODUCTION

Single or multiple lesions of increased radiodensity, defined as "bone islands" (BIs) or enostoses are commonly detected on skeletal radiographs. Enostosis appear radiologically as an avoid, round, or oblong in shape, and they are usually aligned with the long axis of the trabecular architecture.[1,2] BI is one of the most common benign entities that can sometimes be confused with malignancy tumors, in particular in oncological patients.[3] BI is a very frequent incidental finding on CT but the exact frequency is unknown to the best of our knowledge. The classic radiographic features of an enostosis include uniformly radiodense lesion of variable size.[1,2] A diagnosis of BI is essentialy based on imaging findings in the correct clinical context.[4] Plain film radiograph shows a homogeneously dense and sclerotic intramedullary focus with distinctive radiating spicules (referred to as "thorny radiation") at the margins that blend with the neighboring trabeculae of the host bone and resembling a "brush border."[4] Spiculated margin intermingling with thickened

trabeculae without bone destruction, periosteal reaction and soft tissue involvement on CT is diagnostic.[5,6] Any osseous site can be affected, but the lesions have a predilection for the pelvis, proximal femur and ribs.[1,4,5] The increased use of CT scan has led to an increase in the incidental detection bone lesions.[7,8] BI and osteoblastic bone metastases have to be included in the differential diagnosis of newly identified sclerotic osseous lesions,in patients with malignancies.[7,9] The correct characterization of bone lesion is important because can potentially change staging, patient prognosis, and treatment. Indeterminate sclerotic lesions should be evaluated by F-fludeoxyglucose positron emission tomography/CT or bone scintigraphy performed using ^{99m}Tc–methylene diphosphonate.[7] In recent times, Ulano et al[10] proposed a method based on CT attenuation threshold (maximum and mean value) to distinguish BI from untreated osteoblastic metastases (UOM) and showed high accuracy

The purpose of this study is to determine the frequency and density of bone lesions with characteristics of enostosis, incidentally detected on CT, to compare the density values of BI with UOM, and to identify whether CT attenuation threshold could be used for differentiation.

Table 1. History of the 20 patients with UOM

1	06/2014 PET for primitive neoplasm research: lung cancer	07/2014 CT staging: osteoblastic metastases
2	01/2014 mammographic screening, suspicious polymorphic microcalcifications: breast cancer	01/2014 CT staging: osteoblastic metastases
3	2000: right breast cancer operated, 2005: left breast cancer operated	01/2014 bone scintigraphy for rachis pain: osteoblastic metastases 01/2014 PET: osteoblastic metastases
4	2001: prostate cancer operated	10/2014 bone scintigraphy for increased levels of PSA and rachis pain: osteoblastic metastases
5	2010: breast cancer operated	05/2013 CT thorax for fever: osteoblastic metastases
6	02/2015 Ultrasound abdomen in emergency for epigastric pain: hepatic metastases	03/2015 CT total body for primitive neoplasm research: osteoblastic metastases
7	Patient with kidney transpanted (2003) 09/2014 chest X-ray control: pulmonary opacifity	02/2015 CT total body for neoplasm research: osteoblastic metastases
8	2008: right breast cancer operated	06/2014 bone scintigraphy for rachis pain: osteoblastic metastases 06/2014 PET: osteoblastic metastases
9	12/2014 chest X-ray for fever: pulmonary opacity	12/2014 CT thorax: lung cancer with osteoblastic metastases
10	02/2014: URO-TC for hematuria: bladder cancer with osteoblastic metastases	04/2014 bone scintigraphy: osteoblastic metastases
11	04/2014 chest X-ray for fever: pulmonary opacity	05/2014 PET-CT: lung cancer with osteoblastic metastases
12	2005: breast cancer operated	05/2015 bone scintigraphy for control: osteoblastic metastases
13	01/2015 mammographic screening: suspicious breast lump	02/2015 CT total body: osteoblastic metastases
14	07/2013 chest X-ray for severe dyspnea: massive pleural effusion	07/2013 CT thorax: lung cancer with osteoblastic metastases
15	02/2013 mammographic screening: suspicious breast lump	04/2013 bone scintigraphy for staging: osteoblastic metastases
16	02/2015 abdominal ultrasound: bladder cancer	02/2015 bone scintigraphy for staging: osteoblastic metastases
17	10/2014 mammographic screening: suspicious breast lump	10/2014 bone scintigraphy for staging: osteoblastic metastases
18	2006: prostate cancer operated	10/2012 bone scintigraphy for increased levels of PSA and rachis pain: osteoblastic metastases
19	08/2013 mammographic screening: suspicious breast lump	08/2013 bone scintigraphy for staging: osteoblastic metastases
20	09/2013 mammographic screening: suspicious breast lump	09/2013 bone scintigraphy for staging: osteoblastic metastases

UOM, untreated osteoblastic metastases.

Figure 1. Multiplanar evaluation of the BI. BI, bone island.

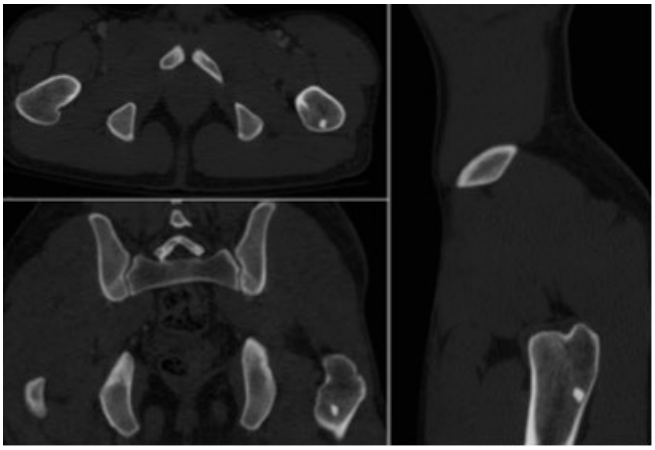

METHODS AND MATERIALS

Study population

In this observational and retrospective study we considered two groups of patients. Enostosis group: from January 2016 to December 2016, 672 patients underwent to thoracoabdominal CT scan for trauma admitted to our emergency department: we identified 46 patients. Inclusion criteria: age range 14–35 years, considering the very low incidence of the most common cancers with osteoblastic metastases (<30 years for females considering breast cancer the most common;<35 years for males considering prostate cancer the most common). Exclusion criteria: known history of malignancy and previous fractures.

UOM group: we identified 20 patients with breast, prostate, lung, bladder and portio cancer, by searching radiology text reports using EL.CO software. The diagnosis was radiological, confirmed by previous studies and radiological appearance during the follow up. Patients were excluded if they started treatment before the first CT available for this study or if the baseline CT was not performed.

It is known that osteoblastic reparative response as a healing reaction during chemotherapy and results in density increase in lesions.[11]

In 18 patients UOM were multiple, in 2 patients a single metastasis. Table 1 shows the radiological history at diagnosis of the 20 patients. In six patients metastases compared during staging CT for breast cancer. In six patients osteoblastic metastases were detected after surgical treatment and in eight patients during CT scan, after incidental cancer diagnosis at XR or abdominal ultrasound.

CT examinations

Lesions were detected using 64-MDCT scanner (LightSpeed, GE Healthcare). All patients underwent thoracoabdominal CT (slice thickness, 2.5 mm for chest, abdomen and pelvis; table feed, 15 mm/s; pitch, 1.5; tube voltage, 120 kVp; tube current 200 mA; sagittal and coronal reconstruction thickness, 2 mm with 2 mm intervals). All patients had intravenous contrast material administrated at rate of 3–4 ml s^{-1} (iomeprolo 350 mg ml^{-1}; Iomeron 350, Bracco Diagnostics). In patients studied with multiphase protocol acquisition measurements ware performed in venous phase.

Figure 2. Measure of the mean attenuation CT of enostosis (a) and UOM (b), the elliptical ROI tool used to draw the largest possible ROI over the lesion without extending beyond the lesion's margins. ROI, region of interest; UOM,untreated osteoblastic metastases.

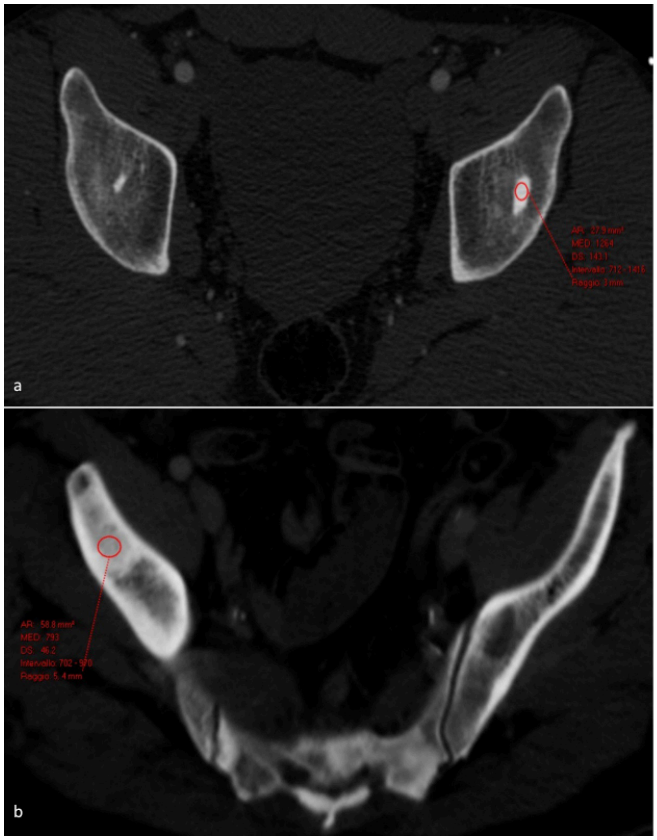

Image analysis

Analyzed data: number, size, location and density (Hounsfield unit, HU) of BI. The density was determined with the broadest possible ROI at the center of the enostosis on the axial or multiplanar images. Attenuation measurements were performed on a PACS workstation (Carestream Health) by two radiologists independently, with more than 15 years experience in CT during multiple separate reading sessions using a picture archiving and with bone settings (window width, 1500 HU; level, 300 HU). Radiologists reviewers were blinded about the group. The measurements were effect on the images acquired in the contrast-enhanced CT studies. The entire study was reviewed, and all lesions with a diameter greater than 2 mm was selected. The target lesion was studied in the axial, coronal, and sagittal planes (Figure 1).

In both groups of patients, the largest cross-sectional area was selected in order to measure the mean attenuation. Elliptical ROI tool was used to draw the largest possible ROI over the target lesion without extending beyond the margins of lesions (Figure 2a–b).

Statistical analysis

The means and standard deviations (SDs) of the density were calculated for the all enostoses within a single patient and for all the UOM within a single patient. Receiver operatingcharacteristic

Table 2. Characteristics of the enostoses

Enostosis	Number per patient	Frequency	Size Mean ± SD (mm)	Density Mean ± SD (HU)
124	• One (13/41) • Two (8/41) • Three (9/41) • > Three (11/41)	41/46 (89%)	4,3 ± 2,4 (range 2–15 mm)	1007 ± 122 1019 ± 105

HU, Hounsfield unit; SD, standard deviation.

(ROC) curves were plotted to determine sensitivity and specificity, area under the curve (AUC), and 95% confidence intervals (CIs) as well as cut-off values of CT attenuation to differentiate metastases from enostoses.

RESULTS

Enostoses group: 46 patients (74% males, 26% females) evaluated, the patient age range was 14–30 years for females and 17–35 years for males (age average 28 ± 7 years). 41 of the 46 patients (89%) had 124 enostoses (2–15 mm), 34/34 males had enostosis, 7/12 females had enostosis (Table 2). No significant differences emerged regarding the number and size of the enostosis between males and females. UOM group was composed by 20 patients (13 females and 7 males). There were 6 patients with lung cancer metastases; 10 with breast cancer metastases; 2 with prostate cancer metastases; 1 with bladder cancer metastases and 1 with portio cancer metastases (Table 3). A total of untreated osteoblastic metastatic lesions identified were 114 (23 lung cancer; 72 breast cancer; 11 prostate cancer; 7 bladder cancer and 1 portio cancer) (Table 3). These lesions were not histologically proven but reasonably confirmed by imaging examinations. One patient (5%) had a negative CT performed 12 years before diagnosis. Six patients (30%) with a primary malignancy previously treated with surgery had several negative follow-up CT before cancer relapse with osteoblastic metastases. In 13 patients (65%) osteoblastic metastases were confirmed by one of two nuclear medicine imaging techniques (bone scintigraphy with 99mTc–methylene diphosphonate and ^{18}F-NAF PET/CT) which are very accurate methods for differentiating enostoses from osteoblastic metastases.[7]

Table 3. Attenuation CT (mean ± SD) of the UOM measured by two radiologists independently

Patient No.	Disease	No.of lesions	SIze Mean ± SD (mm)	Density Mean ± SD (HU) (1°Radiologist)	Density Mean ± SD (HU) (2°Radiologist)
1	Lung cancer	1	9	573	579
2	Breast cancer	10	15 ± 6	785 ± 107	783 ± 113
3	Breast cancer	14	23 ± 8	844 ± 91	861 ± 128
4	Prostate cancer	9	18 ± 11	831 ± 94	816 ± 138
5	Breast cancer	6	20 ± 5	660 ± 95	644 ± 98
6	Lung cancer	3	8 ± 1	454 ± 30	446 ± 24
7	Portio cancer	1	26	502	482
8	Breast cancer	2	24 ± 8	504 ± 2	508 ± 23
9	Lung cancer	3	8 ± 2	577 ± 61	569 ± 82
10	Bladder cancer	3	30 ± 4	585 ± 8	455 ± 35
11	Lung cancer	3	25 ± 8	418 ± 42	391 ± 51
12	Breast cancer	2	24 ± 2	978 ± 16	974 ± 20
13	Breast cancer	11	12 ± 5	555 ± 56	527 ± 42
14	Lung cancer	13	33 ± 16	878 ± 93	856 ± 139
15	Breast cancer	3	25 ± 14	835 ± 12	756 ± 140
16	Bladder cancer	4	29 ± 19	732 ± 110	707 ± 102
17	Breast cancer	7	28 ± 15	692 ± 96	670 ± 105
18	Prostate cancer	2	14 ± 5	668 ± 32	666 ± 23
19	Breast cancer	9	23 ± 8	805 ± 158	757 ± 177
20	Breast cancer	8	21 ± 7	700 ± 129	696 ± 153

HU, Hounsfield unit; SD, standard deviation; UOM, untreated osteoblastic metastases.

Table 4. Attenuation CT (mean ± SD) of the Enostoses measured by two radiologists indipendently

Patient No.	No. of enostoses	Size Mean ± SD (mm)	Density Mean ± SD (HU) (1°Radiologist)	Density Mean ± SD (HU) (2°Radiologist)
1	1	4	831	839
2	1	6	1189	1201
3	2	3 ± 0	1026 ± 146	1021 ± 113
4	2	3 ± 1	1034 ± 128	992 ± 25
5	1	5	1141	1129
6	3	3 ± 2	995 ± 6	1031 ± 65
7	2	3 ± 1	1008 ± 101	987 ± 16
8	3	3 ± 1	945 ± 141	948 ± 139
9	2	2 ± 1	986 ± 145	976 ± 124
10	3	4 ± 1	910 ± 66	907 ± 71
11	1	4	1006	1001
12	3	7 ± 4	1043 ± 90	1056 ± 50
13	4	3 ± 1	954 ± 32	964 ± 34
14	2	4 ± 2	1208 ± 117	1164 ± 48
15	3	4 ± 1	1051 ± 57	1039 ± 55
16	1	3	1001	998
17	3	4 ± 0	974 ± 69	966 ± 62
18	7	5 ± 2	1105 ± 59	1105 ± 46
19	9	5 ± 3	994 ± 92	1017 ± 83
20	3	4 ± 1	949 ± 42	951 ± 40
21	3	2 ± 0	937 ± 11	992 ± 14
22	3	5 ± 1	1092 ± 122	1092 ± 114
23	1	5	957	944
24	2	5 ± 2	929 ± 70	941 ± 38
25	1	6	1110	1103
26	1	3	975	1001
27	12	5 ± 4	1005 ± 164	1028 ± 150
28	5	7 ± 5	1042 ± 146	1054 ± 106
29	1	5	1020	1018
30	7	4 ± 2	1050 ± 170	1054 ± 119
31	4	5 ± 1	868 ± 138	921 ± 99
32	1	4	1136	1129
33	1	6	1104	1098
34	4	3 ± 1	925 ± 178	982 ± 167
35	1	3	1050	1048
36	5	3 ± 1	1033 ± 144	1047 ± 136
37	6	2 ± 1	911 ± 100	939 ± 78
38	2	3 ± 0	1037 ± 40	1041 ± 54
39	1	3	1237	1245

(Continued)

Table 4. (Continued)

Patient No.	No. of enostoses	Size Mean ± SD (mm)	Density Mean ± SD (HU) (1°Radiologist)	Density Mean ± SD (HU) (2°Radiologist)
40	2	5 ± 1	996 ± 7	1003 ± 7
41	5	4 ± 1	1010 ± 115	1033 ± 131

HU, Hounsfield unit; SD, standard deviation; UOM, untreated osteoblastic metastases.

Mean size of BIs was 4.3 ± 2.4 mm (Table 4). The most common sites of occurrence in our study were the proximal femur (34%), the pelvis (22%), the acetabulum (20%), the proximal humerus (11%), the vertebrae (11%) and the rib (2%) (Figure 3). 13 patients had a single BI, 8 patients had two, 9 cases had three and 11 cases had more than three enostoses (Table 2). The BI average density we found was 1007 ± 122 HU for the first radiologist and 1019 ± 105 HU for the second (Table 4), the maximum attenuation value was 1326 ± 8 HU measured in the largest enostosis. The metastases average density measured was 679 ± 156 HU for the first radiologist and 728 ± 196 HU for the second (Table 3), the maximum attenuation value was 976 ± 2 HU in a breast cancer metastasis. ROC curve analysis showed that the mean CT attenuation found can be reliably used to differentiate enostoses from UOM. The AUC value of mean CT attenuation to distinguish enostoses from UOM was 0.9829 (Figure 4). With the Liu test, using a cutoff of 881 HU for mean attenuation, sensitivity was 98%, and specificity was 95%.

DISCUSSION

An enostosis or BI represents a focus of mature compact (cortical) bone within the cancellous bone (spongiosa).[4,10] Some authors consider enostosis as a tumor-like condition, since it consists of a group of normal cells that have proliferated in an abnormal location; by others it is considered a hamartoma, the benign lesion probably congenital or developmental in origin that failed to resorb during endochondral ossification.[2,4,10,12] Usually the size of the enostosis does not change over time, although growth has been documented.[13,14] BI is one of the more common benign bone entities, in our study 41/46 patients (89%) had enostoses, so it is a very frequently finding during CT total body. These patients were all devoid of malignancies, however, when an osteoblastic lesion is identified both in the presence and in the absence of a primary neoplasm, confusion arises. The evaluation of a bone lesion should always be performed in the clinical context, it must also consider the tumor markers and, if it were possible, it should use the comparison with the previous imaging. According to previous studies, the CT attenuation level of the lesion can be further useful for diagnosis, and can avoid additional tests such as biopsy, when the radiological characteristics are not typical, there are no previous examinations useful for comparison and the clinical history is not diriment.[10] The BI average density we found was 1007 ± 122 HU for the first radiologist and 1019 ± 105 HU for the second, the result is comparable to the study of Ulano et al.[10] The metastases average density measured was 679 ± 156 HU for the first radiologist and 728 ± 196 HU for the second. In the UOM group only patients with UOM were included since after chemotherapy and treatment with bisphosphonate therapy, sclerosis may increase as a reparative osteoblastic response and may result in a lesion with a higher CT attenuation, which appears as dense as or even more dense than enostosis.[7,10] Ulano et al also hypothesized that the CT attenuation values of UOM may be tumor-dependent, as in their study, certain lesions secondary to prostate cancer exceeded the attenuation threshold typical of the other metastases evaluated.[10] However, also in our study some UOM exceeded the threshold but it was mostly of breast cancer lesions, in effect the maximum attenuation value was 976 ± 2 HU in a breast cancer metastasis.

Figure 3. The most common sites of the enostoses.

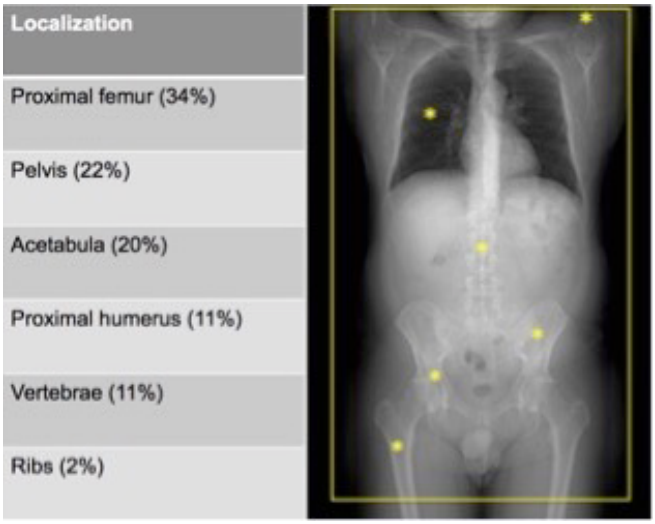

Figure 4. ROC curves for maximum CT attenuation. Graph shows AUC of 0.9829 (*solid line*) for maximum CT attenuation. AUC, area under the curve; ROC, receiver operatingcharacteristic.

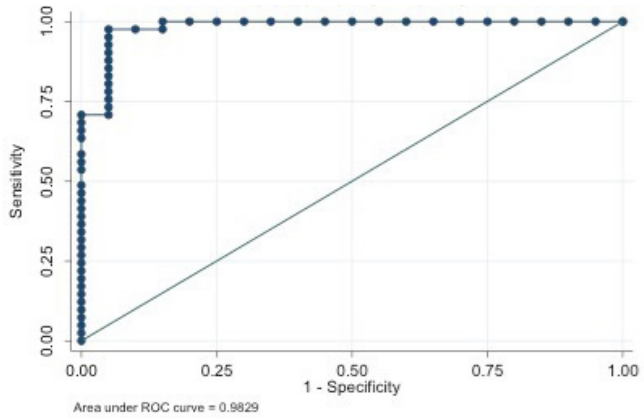

The threshold mean CT attenuation found to distinguish the enostoses from the UOM is very close to that of the previous studies,[7,10] a cutoff of 881 HU had sensitivity 98% and specificity 95%.

Previous studies affirm that BIs are observed in both males and females and in all age groups with probably less frequency in pediatric patients.[1] The patients in this study were 28 ± 7 years old, 34/34 males had enostosis, 7/12 females had enostosis, so we have hypothesized that the enostoses are more frequent in males. However, this statement would require further confirmation with a population that includes an equal number of males and females.

Also the location of the enostoses detected in our study coincides with those reported in the literature. The pelvis, the femur, and other long bones are preferred sites of involvement, BIs can occur anywhere in the skeleton including the ribs and carpal bone, although they are most common in the pelvis, femur and other long bones.[4,5] The spine is more rarely affected**,** Onitsuka has counted only 3 (1.4%) of 209 vertebral BIs and they involved the thoracic and lumbar segments.[13] The most common sites of occurrence in our study were the proximal femur (34%), the pelvis (22%), the acetabulum (20%), the proximal humerus (11%), the vertebrae (11%) and the rib (2%) (Figure 3). 13 patients had a single BI, 8 patients had two, 9 cases had three and 11 cases had more than three enostoses (Table 1).

LIMITATIONS

The main limitations of this study are the retrospective design and the small sample.

None of the lesions have been histologically confirmed. The diagnosis was radiological, confirmed by previous studies and follow-up radiologic appearance. In particular, in the enostoses group the diagnosis has been suggested by radiological features incidentally detected in a young and non-oncologic population during post-trauma evaluation. For this reason such findings should be reasonably considered enostoses.

Moreover, the UOM group is inhomogeneous because of the higher percentage of patient with breast than prostate cancer: this might lead to an underestimation of the reliable threshold of CT attenuation.

CONCLUSIONS

With the increase of the CT examinations, enostoses are more frequently detected than the literature reported by the RX studies alone (1.4%). To the best of our knowledge, the exact frequency is not reported in literature, while in our sample it was 89%. The mean measured density agrees with that of recent studies and may aid in the differential diagnosis with osteoblastic metastases before treatment. BIs are frequent incidental findings and they might be misdiagnosed in oncologic patients. The knowledge of a reliable threshold of CT attenuation is an interesting and potentially useful tool to employ in the early diagnostic and therapeutic management of oncologic patients.

ACKNOWLEDGMENT

FROM - Fondazione per la Ricerca dell'Ospedale di Bergamo kindly provided statistical advice for this manuscript.

REFERENCES

1. Resnick D, Kransdorf M. *Bone and Joint Imaging*: Elsevier; 2005.
2. Di Primio G. Benign spotted bones: a diagnostic dilemma. *Can Med Assoc J* 2011; **183**: 456–9. doi: https://doi.org/10.1503/cmaj.091740
3. Gould CF, Ly JQ, Lattin GE, Beall DP, Sutcliffe JB. Bone tumor mimics: avoiding misdiagnosis. *Curr Probl Diagn Radiol* 2007; **36**: 124–413rd. doi: https://doi.org/10.1067/j.cpradiol.2007.01.001
4. Greenspan A. Bone island (enostosis): current concept--a review. *Skeletal Radiol* 1995; **24**: 111–5. doi: https://doi.org/10.1007/BF00198072
5. Nguyen M, Beaulieu C, Weinstein S, Shin LK. The incidental bone lesion on computed tomography: management tips for abdominal radiologists. *Abdom Radiol* 2017; **42**: 1586–605. doi: https://doi.org/10.1007/s00261-016-1040-0
6. Ehara S, Kattapuram SV, Rosenberg AE. Giant bone island. computed tomography findings. *Clin Imaging* 1989; **13**: 231–3. doi: https://doi.org/10.1016/0899-7071(89)90154-X
7. Elangovan SM, Sebro R. Accuracy of CT attenuation measurement for differentiating treated osteoblastic metastases from Enostoses. *AJR Am J Roentgenol* 2018; **210**: 615–20. doi: https://doi.org/10.2214/AJR.17.18638
8. Berland LL, Silverman SG, Gore RM, Mayo-Smith WW, Megibow AJ, Yee J, et al. Managing incidental findings on abdominal CT: white paper of the ACR incidental findings Committee. *J Am Coll Radiol* 2010; **7**: 754–73. doi: https://doi.org/10.1016/j.jacr.2010.06.013
9. Greenspan A, Jundt G, Remagen W. *Differential diagnosis in orthopaedic oncology*. 2rd edn. Philadelphia: Lippincott Williams & Wilkins; 2007.
10. Ulano A, Bredella MA, Burke P, Chebib I, Simeone FJ, Huang AJ, et al. Distinguishing untreated osteoblastic metastases from Enostoses using CT attenuation measurements. *AJR Am J Roentgenol* 2016; **207**: 362–8. doi: https://doi.org/10.2214/AJR.15.15559
11. Stattaus J, Hahn S, Gauler T, Eberhardt W, Mueller SP, Forsting M, et al. Osteoblastic response as a healing reaction to chemotherapy mimicking progressive disease in patients with small cell lung cancer. *Eur Radiol* 2009; **19**: 193–200. doi: https://doi.org/10.1007/s00330-008-1115-6
12. Avila NA, Dwyer AJ, Rabel A, Darling T, Hong C-H, Moss J. Ct of sclerotic bone lesions: imaging features differentiating tuberous sclerosis complex with lymphangioleiomyomatosis from sporadic lymphangioleiomymatosis. *Radiology* 2010; **254**: 851–7. doi: https://doi.org/10.1148/radiol.09090227
13. Onitsuka H. Roentgenologic aspects of bone islands. *Radiology* 1977; **123**: 607–12. doi: https://doi.org/10.1148/123.3.607
14. Blank N, Lieber A. The significance of growing bone islands. *Radiology* 1965; **85**: 508–11. doi: https://doi.org/10.1148/85.3.508